PHYSICAL REVIEW D **87,** 063520 (2013)

Nonlinear evolution of cosmological structures in nonthermal production of dark matter model

Y. He and W. Lin*

School of Physical Science and Technology, Southwest Jiaotong University, Chengdu 610031, China

(Received 30 January 2013; published 21 March 2013)

The nonthermal production of dark matter can provide a large free-streaming length, under which the density fluctuations would be suppressed severely. We explore the nonlinear evolution of cosmological structures in the dark energy dominated model with nonthermal dark matter (NTDM). With the help of *N*-body simulations, we study the nonlinear matter power spectrum, the halo mass function, and the halo density profiles. It is demonstrated that NTDM produces a far lesser number of the subgalactic structures than that of the conventional cold dark matter (CDM). We also find that the density profiles of the low-mass halos in the NTDM model are flat, in contrast to the cuspy cores predicted by the CDM model. The *N*-body simulations show that the inconsistent predictions of the standard model on the galactic and subgalactic scales may be accounted for by the nonthermal mechanism for the production of dark matter.

DOI: 10.1103/PhysRevD.87.063520 PACS numbers: 98.80.−k, 95.35.+d, 98.62.Gq

I. INTRODUCTION

The dark energy dominated cold dark matter (CDM) scenario has been a standard model for cosmology, whose predictions are in good agreement with the observations of the large scale structures and the cosmic microwave background [1–3]. However, there are some discrepancies between its predictions and the observations of the galactic and subgalactic scales. For example, the amount of subgalactic structures is overpredicted by roughly 1 order of magnitude in the CDM models [4–6]. Secondly, the inner density profiles of halos in CDM simulations are much sharper than the observations [7–14].

In order to resolve these discrepancies, Spergel and Steinhardt proposed that these conflicts can be alleviated if the dark matter particles have self-interactions with a large scattering cross section but negligible annihilation or dissipation [15–19]. Another alternative solution is warm dark matter (WDM) [20–24]. The candidates for conventional WDM are sterile neutrinos [25,26] and gravitinos [27–29]. Recently, there have been a number of studies on the nonlinear evolution for the WDM model at galactic scales [30–36].

The leading candidates for dark matter are weakly interacting massive particles (WIMPs), such as the neutralino [37–40]. In the models with *R* parity, the neutralino is stable, and its mass density in the Universe is generally assumed to be a relic of an initially thermal distribution in the hot early Universe. However, the neutralino might be produced via a nonthermal mechanism [41,42]. For simplicity, the dark matter which has nonthermal production origins is referred to as nonthermal dark matter (NTDM) below. We have shown that the linear matter power spectrum of the NTDM can be lower than that of the conventional CDM on subgalactic scales, and it provides a promising solution to the discrepancies at subgalactic scales for the standard model [43]. On the other hand, the NTDM scenario has some interesting properties in the search for dark matter [44,45]. During the direct and indirect detections, the strength of signal depends upon the density of dark matter and the space distribution. Recently both PAMELA and FERMI reported excesses in the cosmic ray positrons and gamma rays above the anticipated astrophysical backgrounds. These excesses might favor the nonthermal origin of dark matter, which has a large self-annihilation cross section [46–48]. Over the last decade, the nonthermal dark matter scenario has been extensively studied by many groups [49–51].

Although we have shown that the linear matter power spectrum of the NTDM model exhibits lower amplitudes than those of the CDM model on the small scales, the detailed effects of the nonthermal production of dark matter in the formation of galactic and subgalactic halos needs further study. In this paper we explore the nonlinear evolution of the structure formation in the NTDM scenario via an ensemble high-resolution *N*-body simulations. We investigate the nonlinear matter power spectrum, the halo mass function, and the halo density profiles, and we make comparisons to those from the CDM model as well as the WDM model.

This paper is organized as follows: Sec. II gives an overview of the nonthermal dark matter. In Sec. III we explore the nonlinear evolution of large-scale structure in the NTDM scenario. Discussions and conclusions are given in Sec. IV.

II. THE NTDM MODEL

In the canonical WIMPs paradigm, dark matter is assumed to be produced thermally in the early Universe. The velocities of the WIMPs are nonrelativistic after

---

*wl@swjtu.edu.cn

decoupling and thus they behave like CDM. Alternatively, if they are produced nonthermally, WIMPs could behave like WDM. Their comoving free-streaming scale could be as large as the order of 0.1 Mpc or larger, within which the density fluctuations would be suppressed severely. We have demonstrated that the linear matter power spectrum of the NTDM model has much lower amplitudes on the small scales, compared to those of the CDM model [43].

In this paper, we further explore the nonlinear evolution of the NTDM in the model presented in Ref. [43], in which the momentum distribution function of the neutralinos is assumed to be Gaussian:

$$f(p) = \frac{A}{\sqrt{2\pi}\sigma} \exp\left[-\frac{(p-p_c)^2}{2\sigma^2}\right], \tag{1}$$

where p_c and σ denote the central value and the width of the distribution. In this case, the comoving free-streaming scale λ_{fs} for the nonthermal particles can be estimated by [43,52,53]

$$\lambda_{fs} \approx 2r_c t_{\mathrm{EQ}}(1+z_{\mathrm{EQ}})^2 \times \ln\left(\sqrt{1+\frac{1}{r_c^2(1+z_{\mathrm{EQ}})^2}} + \frac{1}{r_c(1+z_{\mathrm{EQ}})}\right), \tag{2}$$

where t_{EQ} and z_{EQ} denote the redshift and the time for radiation-matter equality, and r_c represents the central value for the comoving velocities of the neutralinos. We have shown that the linear matter power spectrum of the NTDM model with $r_c \sim 10^{-7}$ has similar amplitudes as those of the fully thermalized WDM model with $m_{\mathrm{WDM}} \sim 1$ keV on the galactic scales, and this may account for the inconsistencies of the conventional CDM model.

Notice that some works show that the sterile neutrino mass m_{ν_s} has to be larger than 10 keV; for example, see Ref. [54]. But more recently, lower bounds (e.g., $m_{\nu_s} >$ 2 keV) have also been considered for the sterile neutrino by many groups [33,34,36,51,55–58]. The mass m_{ν_s} of the sterile neutrino can be related to the mass m_{WDM} of the fully thermalized WDM through the formula given by Viel *et al.* [55]:

$$m_{\nu_s} = 4.43\ \mathrm{keV}\left(\frac{m_{\mathrm{WDM}}}{1\ \mathrm{keV}}\right)^{4/3}\left(\frac{w_{\mathrm{WDM}}}{0.1225}\right)^{-1/3}, \tag{3}$$

with the WDM density parameter $w_{\mathrm{WDM}} \sim 0.12$. Thus, the bound $m_{\nu_s} > 2$ keV for the sterile neutrino is equivalent to $m_{\mathrm{WDM}} > 0.55$ keV for thermalized WDM. Specifically, Schneider *et al.* perform a set of high-resolution N-body simulations for WDM with $m_{\mathrm{WDM}} = \{0.25\ \mathrm{keV}, 0.5\ \mathrm{keV}, 0.75\ \mathrm{keV}, 1.0\ \mathrm{keV}, 1.25\ \mathrm{keV}\}$ to study the nonlinear evolution of cosmological structures [36]. In this work, we pick $m_{\mathrm{WDM}} = 0.75$ keV, the middle value of the WDM masses they consider, as an example for comparison.

III. NONLINEAR EVOLUTION FOR STRUCTURES IN THE NTDM MODEL

We consider a flat dark energy and a NTDM dominated model. Based on the data provided in Ref. [3], the cosmological parameters are chosen as follows: $\Omega_m = 0.28$, $\Omega_\Lambda = 0.72$, $\Omega_b = 0.046$, $h = 0.7$, $n_s = 0.97$, $\sigma_8 = 0.82$, where Ω_Λ, Ω_b are the ratios of the contributions of the total matter, dark energy, and baryons to the total density of the Universe. h is the dimensionless Hubble parameter. n_s is the primordial power spectral index, and σ_8 denotes the fluctuations at the scale of 8 h^{-1} Mpc.

Figure 1 shows the linear power spectrum of this model with $r_c = 0.66 \times 10^{-7}$. For comparison, we also show the power spectra for the conventional CDM model and the WDM model with $m_{\mathrm{WDM}} = 0.75$ keV. It can be seen that the three power spectra are the same on large scales, and the power spectrum of the NTDM model is damped severely relative to that of the CDM model on the galactic and subgalactic scales, similar to that of the WDM model.

In order to obtain the nonlinear evolution for the large-scale structures in the NTDM model, we employ the GADGET-2 [59] to do N-body simulations [60]. The initial condition at high redshift (e.g., $z = 49$) is determined by the linear power spectrum. We apply the second-order Lagrangian perturbation theory to obtain the initial positions and velocities of particles [61,62], using the 2LPT code [63] with a "glass" initial particle load [64]. For all runs, we set the box length $L_{\mathrm{box}} = 64\,\mathrm{h}^{-1}$ Mpc and the total number of particles $N = 256^3$. The mass of each particle is $5.95 \times 10^8\ \mathrm{h}^{-1} M_\odot$, and the force softening is 5 h^{-1} kpc.

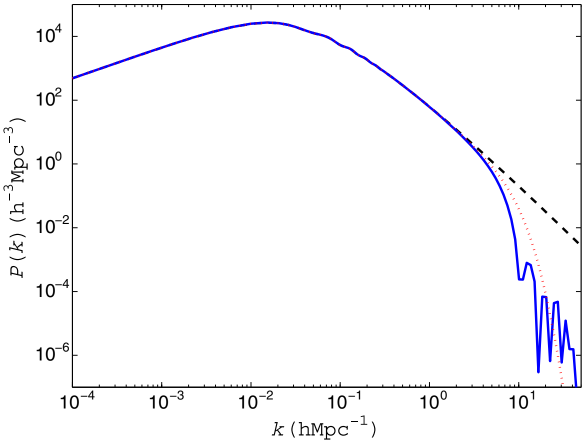

FIG. 1 (color online). Comparison of the linear matter power spectra of the NTDM model with $r_c = 0.66 \times 10^{-7}$ (solid blue line), the CDM model (long-dashed black line), and the WDM model with $m_{\mathrm{WDM}} = 0.75$ keV (short-dashed red line).

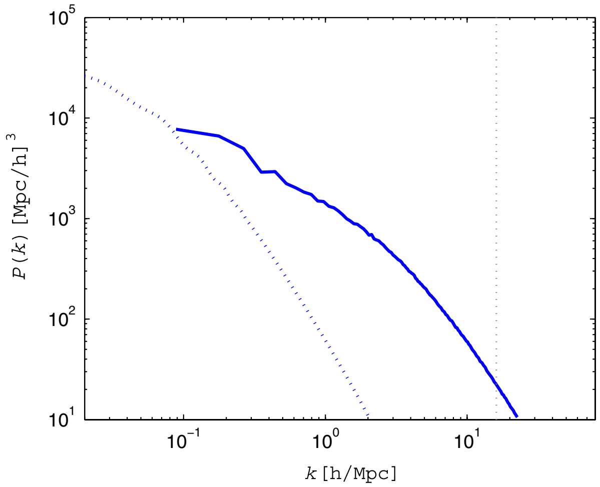

FIG. 2 (color online). Comparison between the nonlinear power spectrum (solid blue line) deduced from the N-body simulations and the linear matter power spectrum (dotted blue line). The vertical gray dots indicate half the Nyquist frequency.

A. Nonlinear matter power spectrum

With the N-body simulation results, we can apply the POWMES code [65] to calculate the nonlinear power spectrum. The code is based on the Taylor expansion of the trigonometric functions [66]. Figure 2 shows the nonlinear matter power spectra at redshift $z = 0$ for the NTDM model. For comparison, the linear matter power spectrum is also shown. We can see that the differences between the nonlinear and linear matter power spectra are huge on the small scales, and this implies that nonlinear evolution plays a very crucial role in the formation of the small-scale structures, such as subgalactic halos.

Figure 3 gives the comparisons of the nonlinear matter power spectra at redshift $z = 0$ for the NTDM model, the conventional CDM model, and the WDM model. It can be seen from this figure that there is little difference among these three power spectra on the scales with $k \leq 1\ \mathrm{h\,Mpc}^{-1}$. For the small scales, e.g., $k > 1\ \mathrm{h\,Mpc}^{-1}$, we can see that the NTDM power spectrum is suppressed with respect to the CDM one, and it behaves like the WDM. The bottom panel quantifies this suppression in greater detail. For example, for $k \sim 10\ \mathrm{h\,Mpc}^{-1}$, there is about a 15% suppression in power for both the NTDM model and the WDM model.

B. Halo model ingredients

In this section, we investigate the halo mass function and the halo density profiles for the NTDM model. We identified the halos and their subhalos by the AMIGA Halo Finder (AHF) code [67]. The AHF probes the halos at each density peak using a spherical overdensity algorithm [68]. In this work, the criterion for identifying a halo is chosen so that the ratio of its interior density to the mean background density is larger than 200. Moreover, we only keep the halos with at least 20 dark matter particles; i.e., the minimum mass of halos is around $8 \times 10^9\ \mathrm{h}^{-1} M_\odot$.

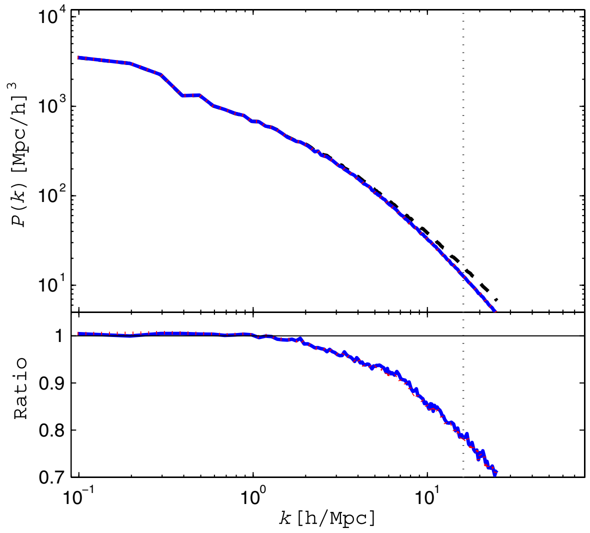

FIG. 3 (color online). Comparison of the nonlinear matter power spectra among the NTDM, CDM, and WDM models. Top panel: The long-dashed black line denotes the CDM power spectrum, the short-dashed red line corresponds to the WDM, and the solid blue line is for the NTDM. Bottom panel: The solid blue line corresponds to the ratio of the power spectra between the NTDM and the CDM, and the short-dashed red line corresponds to the ratio between the WDM and the CDM. The vertical, dotted gray line indicates half the Nyquist frequency.

1. The halo mass function

The halo mass function provides a wealth of information about the formation of structures. We consider the cumulative mass function, which is defined as the mean number densities of the halos with mass larger than a specific mass [69,70],

$$n(>M) = \int_M^\infty f(\sigma) \frac{\bar{\rho}(z=0)}{M} \frac{d \ln \sigma^{-1}}{dM} dM, \tag{4}$$

where $\bar{\rho}$ is the mean background density, and $f(\sigma)$ is the halo multiplicity function.

In Fig. 4 we show the cumulative halo mass function at redshift $z = 0$ in the NTDM model, as well as those of the CDM model and the WDM model with $m_{\mathrm{WDM}} = 0.75$ keV. It can be seen that these mass functions are almost the same for the large masses, e.g., $M > 10^{12}\ \mathrm{h}^{-1} M_\odot$. However, the discrepancies increase as the masses get smaller. In the bottom panel we can clearly see that the NTDM scenario exhibits a strong suppression for $M < 10^{12}\ \mathrm{h}^{-1} M_\odot$ compared to the CDM model, and this is

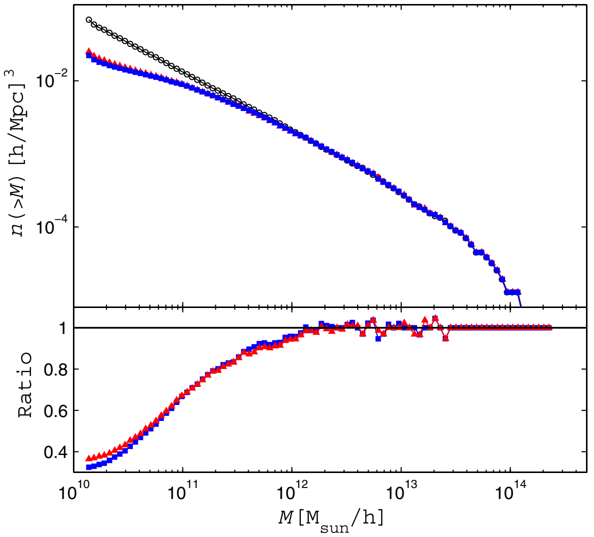

FIG. 4 (color online). The number density of halos greater than a given mass from the simulations. Top panel: Black circles are for the CDM model, blue squares are for the NTDM model, and red triangles are for the WDM model. Bottom panel: Blue squares denote the ratio of $n_{\rm NTDM}(>M)$ to $n_{\rm CDM}(>M)$; red triangles denote the ratio of $n_{\rm WDM}(>M)$ to $n_{\rm CDM}(>M)$.

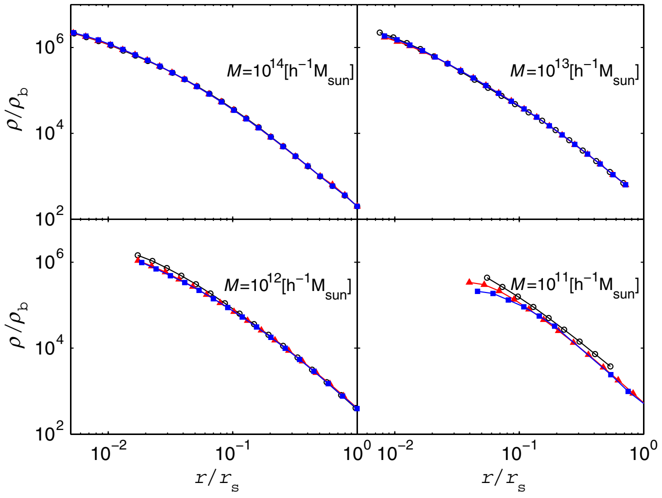

FIG. 5 (color online). Density profiles of the three different dark matter halos as a function of radius. The top left, top right, bottom left, and bottom right panels show the results for the halos with masses $M \in \{10^{14}, 10^{13}, 10^{12}, 10^{11}\}$ h$^{-1}M_\odot$, respectively. In all panels, black circles denote the CDM profiles, blue squares are for the NTDM profiles, and red triangles correspond to the WDM profiles.

consistent with the suppression in the linear power spectrum (see Fig. 1). From Fig. 4 we can also see that the cumulative mass function predicted by the NTDM model is very close to that of the WDM model.

2. The halo density profiles

The density profiles of dark matter halos have been extensively studied, and they can be described by the NFW profiles [7,71]:

$$\frac{\rho(r)}{\bar{\rho}} = \frac{\delta_s}{y(1+y)^2}; \qquad y \equiv \frac{r}{r_s}, \tag{5}$$

where $\delta_{\rm s}$ and $r_{\rm s}$ represent a characteristic overdensity and scale radius.

Because of the suppression of the power spectrum on the small scales, the collapse times of the halos could be significantly affected. For a given halo of mass M, it will collapse at a later time in the NTDM model compared to one in the CDM model. The halo core density is related to the density of the Universe at the collapse time; we may expect that the core densities in the NTDM model will be suppressed, and the halos on average will be less concentrated, than in the WDM scenario [32–36]. This argument is verified by our N-body simulations. Figure 5 shows the density profiles of the halos in the NTDM model. Here the radial distributions of mass in the halos are obtained from four randomly chosen halos of different masses at redshift $z = 0$. For comparison, the corresponding results for the CDM and WDM models are also given. We can see that these profiles cannot be distinguished for high masses. However, the NTDM model exhibits a net flattening in the inner radius for the low masses, e.g., $M \sim 10^{11}$ h$^{-1}M_\odot$, similar to that of the WDM model. Therefore, the cuspy problem about the density profiles in the CDM model may be avoided in the NTDM model.

IV. DISCUSSION AND CONCLUSIONS

With the aid of N-body simulations, we have explored the nonlinear evolution of cosmological structures in the NTDM model, and presented comparisons with the conventional CDM model and the thermal WDM model. We examined the impact of the nonthermal production of dark matter on the nonlinear matter power spectrum and the clustering properties of large-scale structure. Numerical simulations show that the NTDM model can provide the nonlinear suppression for the matter power spectrum on small scales and produce a far lesser number of subgalactic structures than that of the CDM model, as the linear matter power spectrum of the NTDM model suggested.

On the other hand, the nonlinear suppression in the NTDM scenario may also delay the formation of halos. Since the halo core density is related to the density of the Universe when halos form, the cores of low-mass halos in the NTDM model will become less cuspy than those of the CDM model. With the N-body simulations, we verify that the cores of low-mass halos in the NTDM model are very flat compared to those of the CDM model. These flat cores may indicate a top-down formation for the large-scale structures in the NTDM model.

In summary, the N-body simulations demonstrate that the discrepancies between the theoretical predictions of the standard cosmological model and the observations on the galactic and subgalactic scales may be avoided, if the WIMP dark matter is produced via a nonthermal mechanism.

ACKNOWLEDGMENTS

This work was supported in part by the Program for New Century Excellent Talents in University (Grant No. NCET-10-0702), the National Basic Research Program of China (973 Program) Grant No. 2013CB328904, and the Ph.D. Programs Foundation of Ministry of Education of China (Grant No. 20110184110016).

[1] S. Cole, W. J. Percival, J. A. Peacock *et al.* (The 2dFGRS Team), Mon. Not. R. Astron. Soc. **362**, 505 (2005).
[2] M. Tegmark *et al.* (The SDSS Team), Phys. Rev. D **74**, 123507 (2006).
[3] E. Komatsu, K. M. Smith, J. Dunkley *et al.* (The WMAP Team), Astrophys. J. Suppl. Ser. **192**, 18 (2011).
[4] A. Klypin, A. V. Kravtsov, O. Valenzuela, and F. Prada, Astrophys. J. **522**, 82 (1999).
[5] B. Moore, T. Quinn, F. Governato, J. Stadel, and G. Lake, Mon. Not. R. Astron. Soc. **310**, 1147 (1999).
[6] P. J. E. Peebles and A. Nusser, Nature (London) **465**, 565 (2010).
[7] J. F. Navarro, C. S. Frenk, and S. D. M. White, Astrophys. J. **490**, 493 (1997).
[8] S. Ghigna, B. Moore, F. Governato, G. Lake, T. Quinn, and J. Stadel, Astrophys. J. **544**, 616 (2000).
[9] J. Diemand, B. Moore, and J. Stadel, Mon. Not. R. Astron. Soc. **353**, 624 (2004).
[10] J. Stadel, D. Potter, B. Moore, J. Diemand, P. Madau, M. Zemp, M. Kuhlen, and V. Quilis, Mon. Not. R. Astron. Soc. **398**, L21 (2009).
[11] R. A. Swaters, B. F. Madore, F. C. van den Bosch, and M. Balcells, Astrophys. J. **583**, 732 (2003).
[12] P. Salucci, A. Lapi, C. Tonini, G. Gentile, I. Yegorova, and U. Klein, Mon. Not. R. Astron. Soc. **378**, 41 (2007).
[13] W. J. G. de Blok, F. Walter, E. Brinks, C. Trachternach, S.-H. Oh, and R. C. Kennicutt, Jr., Astron. J. **136**, 2648 (2008).
[14] G. Gentile, B. Famaey, H. Zhao, and P. Salucci, Nature (London) **461**, 627 (2009).
[15] D. N. Spergel and P. J. Steinhardt, Phys. Rev. Lett. **84**, 3760 (2000).
[16] N. Yoshida, V. Springel, S. D. M. White, and G. Tormen, Astrophys. J. **544**, L87 (2000).
[17] P. Colin, V. Avila-Reese, O. Valenzuela, and C. Firmani, Astrophys. J. **581**, 777 (2002).
[18] N. Arkani-Hamed, D. P. Finkbeiner, T. R. Slatyer, and N. Weiner, Phys. Rev. D **79**, 015014 (2009).
[19] M. R. Buckley and P. J. Fox, Phys. Rev. D **81**, 083522 (2010).
[20] J. R. Bond and A. S. Szalay, Astrophys. J. **274**, 443 (1983).
[21] J. M. Bardeen, J. R. Bond, N. Kaiser, and A. S. Szalay, Astrophys. J. **304**, 15 (1986).
[22] P. Colin, V. Avila-Reese, and O. Valenzuela, Astrophys. J. **542**, 622 (2000).
[23] J. Sommer-Larsen and A. Dolgov, Astrophys. J. **551**, 608 (2001).
[24] P. Bode, J. P. Ostriker, and N. Turok, Astrophys. J. **556**, 93 (2001).
[25] S. Dodelson and L. M. Widrow, Phys. Rev. Lett. **72**, 17 (1994).
[26] M. Shaposhnikov and I. Tkachev, Phys. Lett. B **639**, 414 (2006).
[27] J. Ellis, J. S. Hagelin, D. V. Nanopoulos, K. Olive, and M. Srednicki, Nucl. Phys. **B238**, 453 (1984).
[28] T. Moroi, H. Murayama, and M. Yamaguchi, Phys. Lett. B **303**, 289 (1993).
[29] D. Gorbunov, A. Khmelnitsky, and V. Rubakov, J. High Energy Phys. 12 (2008) 055.
[30] P. Colin, O. Valenzuela, and V. Avila-Reese, Astrophys. J. **673**, 203 (2008).
[31] J. Zavala, Y. P. Jing, A. Faltenbacher, G. Yepes, Y. Hoffman, S. Gottlöber, and B. Catinella, Astrophys. J. **700**, 1779 (2009).
[32] A. V. Macciò and F. Fontanot, Mon. Not. R. Astron. Soc. **404**, L16 (2010).
[33] M. Lovell, V. Eke, C. Frenk, L. Gao, A. Jenkins, T. Theuns, J. Wang, S. White, A. Boyarsky, and O. Ruchayskiy, Mon. Not. R. Astron. Soc. **420**, 2318 (2012).
[34] M. Viel, K. Markovic, M. Baldi, and J. Weller, Mon. Not. R. Astron. Soc. **421**, 50 (2012).
[35] R. M. Dunstan, K. N. Abazajian, E. Polisensky, and M. Ricotti, arXiv:1109.6291.
[36] A. Schneider, R. E. Smith, A. V. Macciò, and B. Moore, arXiv:1112.0330 [Mon. Not. R. Astron. Soc. (to be published)].
[37] H. Goldberg, Phys. Rev. Lett. **50**, 1419 (1983).
[38] J. R. Ellis, J. S. Hagelin, D. V. Nanopoulos, K. A. Olive, and M. Srednicki, Nucl. Phys. **B238**, 453 (1984).
[39] G. Jungman, M. Kamionkowski, and K. Griest, Phys. Rep. **267**, 195 (1996).
[40] L. Bergström, Rep. Prog. Phys. **63**, 793 (2000).
[41] R. Jeannerot, X. Zhang, and R. H. Brandenberger, J. High Energy Phys. 12 (1999) 003.
[42] D. Chung, E. W. Kolb, and A. Riotto, Phys. Rev. D **59**, 023501 (1998).
[43] W. B. Lin, D. H. Huang, X. Zhang, and R. H. Brandenberger, Phys. Rev. Lett. **86**, 954 (2001).
[44] S. Watson, arXiv:0912.3003.
[45] P. Grajek, G. Kane, D. J. Phalen, A. Pierce, and S. Watson, arXiv:0807.1508.

[46] G. Kane, R. Lu, and S. Watson, Phys. Lett. B **681**, 151 (2009).

[47] P. Grajek, G. Kane, D. Phalen, A. Pierce, and S. Watson, Phys. Rev. D **79**, 043506 (2009).

[48] M. Nagai and K. Nakayama, Phys. Rev. D **78**, 063540 (2008).

[49] B. S. Acharya, G. Kane, S. Watson, and P. Kumar, Phys. Rev. D **80**, 083529 (2009).

[50] X. Bi, R. Brandenberger, P. Gondolo, T. Li, Q. Yuan, and X. Zhang, Phys. Rev. D **80**, 103502 (2009).

[51] Q. Yuan, Y. Cao, J. Liu, P. Yin, L. Gao, X. Bi, and X. Zhang, Phys. Rev. D **86**, 103531 (2012).

[52] E. W. Kolb and M. S. Turner, *The Early Universe* (Addison-Wesley, Redwood City, California, 1993).

[53] S. Borgani, A. Masiero, and M. Yamaguchi, Phys. Lett. B **386**, 189 (1996).

[54] N. Yoshida, A. Sokasian, and L. Hernquist, Astrophys. J. **591**, L1 (2003).

[55] M. Viel, J. Lesgourgues, M. G. Haehnelt, S. Matarrese, and A. Riotto, Phys. Rev. D **71**, 063534 (2005).

[56] A. Knebe, B. Arnold, C. Power, and B. K. Gibson, Mon. Not. R. Astron. Soc. **386**, 1029 (2008).

[57] A. Boyarsky, J. Lesgourgues, O. Ruchayskiy, and M. Viel, Phys. Rev. Lett. **102**, 201304 (2009).

[58] R. E. Smith and K. Markovic, Phys. Rev. D **84**, 063507 (2011).

[59] Available at http://www.mpa-garching.mpg.de/gadget.

[60] V. Springel, Mon. Not. R. Astron. Soc. **364**, 1105 (2005).

[61] R. Scoccimarro, Mon. Not. R. Astron. Soc. **299**, 1097 (1998).

[62] M. Crocce, S. Pueblas, and R. Scoccimarro, Mon. Not. R. Astron. Soc. **373**, 369 (2006).

[63] Available at http://cosmo.nyu.edu/roman/2LPT.

[64] S. D. M. White, in *Cosmology and Large-Scale Structure,* edited by R. Schaefer, J. Silk, M. Spiro, and J. Zinn-Justin (Elsevier, Amsterdam, 1996).

[65] Available at http://www.projet-horizon.fr.

[66] S. Colombi, A. H. Jaffe, D. Novikov, and C. Pichon, arXiv:0811.0313 [Mon. Not. R. Astron. Soc. (to be published)].

[67] Available at http://popia.ft.uam.es/AMIGA.

[68] S. R. Knollmann and A. Knebe, Astrophys. J. Suppl. Ser. **182**, 608 (2009).

[69] W. H. Press and P. Schechter, Astrophys. J. **187**, 425 (1974).

[70] J. R. Bond, S. Cole, G. Efstathiou, and N. Kaiser, Astrophys. J. **379**, 440 (1991).

[71] B. Moore, T. Quinn, F. Governato, J. Stadel, and G. Lake, Mon. Not. R. Astron. Soc. **310**, 1147 (1999).